

FRACTAL AND FREQUENCY BASED ANALYSIS OF ROUGH SURFACES PRODUCED BY DIFFERENT MACHINING OPERATIONS ON HARDENED ALLOY STEEL PARTS

Krzysztof Żak

Summary

The paper presents an original approach to the characterization of the surface profiles/surface topographies produced on hardened steel parts using CBN tools. The experimental investigations involve recording of surface profiles and surface topographies for three different machining operations, namely hard turning, ball burnishing and superfinish in order to obtain a comparable value of the S_a (R_a) parameter of $0.2 \mu\text{m}$. Both fractal and frequency analysis were performed in order to obtain the fractal dimension (S_{fd}) and the signal amplitude and the wavelength which were estimated from the power spectral density (PSD) spectra. The correlations between the S_z (S_a) roughness parameter and the fractal dimension were documented as well as appropriate relations with the frequency characteristics. In particular, the multi-fractal approach to the complex machined surfaces was discussed.

Keywords: fractal and frequency analysis, surface profiles/surface topographies, machining operations, hardened steel

Analiza topografii powierzchni utwardzonej stali stopowej metodami analizy fraktalnej i częstotliwościowej po różnych sposobach obróbki

Streszczenie

W artykule przedstawiono opracowane nowe podejście do charakterystyki profili powierzchni/topografii powierzchni hartowanych stalowych elementów maszyn obrabianych przy użyciu narzędzi CBN. Badania eksperymentalne obejmowały określenie profili powierzchni i topografii powierzchni dla trzech różnych operacji obróbki – toczenia na twardo, nagniatania i dogładzania oscylacyjnego w celu uzyskania porównywalnej wartości parametru S_a (R_a) – $0,2 \mu\text{m}$. Analizę fraktalną i częstotliwościową prowadzono dla ustalenia wymiaru fraktalnego (S_{fd}) oraz amplitudy sygnału i długości fali. Zostały oszacowane na podstawie gęstości widmowej mocy (PSD). Określono korelację pomiędzy parametrem chropowatości S_z (S_a) i wymiarem fraktalnym. Także ustalono ich zależności od charakterystyk częstotliwości. W szczególności uwzględniono w prowadzonej analizie multifraktalne podejście dla powierzchni złożonych.

Słowa kluczowe: analiza fraktalna i częstotliwościowa, profil powierzchni/topografia powierzchni, obróbka skrawaniem, stal utwardzona

1. Introduction

Rapid development of automotive, aircraft and aerospace industry branches observed in XXI century confirmed indicated that the geometrical structure of engineered surfaces influence substantially the functional performance of highly loaded, wear and corrosion resistant machine parts. In particular, it is documented that this influence is of a complex nature because the surfaces produced have a random structure due to many process distributions, which typically deteriorate their regularity. As a result, measured surfaces should be characterized using several group of 2D and 3D surface roughness parameters, not only some frequently used height (Rz/Sz) or amplitude (Sa/Ra) parameters [1].

It is obviously known in engineering practice that measurements and exploitation tests are performed for many specific tasks taking into account such functional correlations, as:

- friction and wear of the mated surfaces;
- contact deformation and joint stiffness
- internal stresses and their concentration;
- corrosion resistance;
- sealing abilities;
- adhesion and bonding abilities of deposited coatings;
- aero- and hydrodynamic properties.

In general, as mentioned above, characterization of geometrical structure of engineered surfaces can be strongly corresponded to their functional performance which depend on the machining operation or the chain of machining operations employed [1-5]. Despite the standard approach using a number of surface roughness parameters the fractal analysis seems to be effective in such cases when the surfaces are similar independently of the observation scale (Fig. 1). The features of similarity can be expressed quantitatively by means of 2D or 3D fractal dimension (D , Sfd) [6,7].

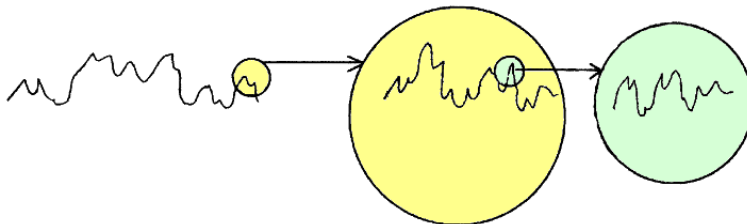


Fig. 1. Illustration of „self-similarity” features, based on [7]

Due to a large variety of fractals its mathematical definition is rather not possible but it is defined as a set which is characterized by the following features[8]:

- has complex structure in each scale,
- its structure is not simply described in Euclidean geometry,
- is self-similar, if not accurately, but approximately or stochastically,
- its Hausdorff's dimension is higher than the topological dimension,
- has relatively simple recurrent definition,
- has *natural* ("sharp", "vermicular" etc.) image.

The value of fractal dimension varies from $D = 1$ to $D = 2$, which means that 1 corresponds to a straight line between two defined points (two-dimensional analysis) whereas value 2 (three-dimensional analysis) defines the space within the straight line is displaced into an arbitrary location. This means that fractals are able to represent and characterize some different shapes [7]. In consequence, although the description of real surfaces by means of fractals is independent of the measuring scale it provides a very valuable information on the structure of surfaces with fractal features [4, 9].

Similarly, the frequency analysis based on the power spectral analysis (PSD) is an effective engineering tool allowing the detection of different distributions generated in the technological system (machine tool-clamping device-cutting tool) which influence the real surface profile/topography. In particular, such negative process interactions as cutting vibrations or workpiece run-outs can be recognized. The frequency analysis is performed using the FFT transform in the domain of frequency wavelength or time.

2. Workpiece material, tooling and machining conditions

Experimental investigations were performed on a 41Cr4 (AISI 5140 equivalent) steel specimens hardened to 57 ± 1 HRC. Machined surfaces were generated using CBN cutting tool inserts of CB 7015 grade, TNGA 160408 S01030 type produced by Sandvik Coromant.

Machining conditions selected for the three machining operations are specified in Table 1.

Table 1. Specification of machining conditions

Symbol of machining operation	Type of machining operation	Machining conditions
<i>Finish turning</i> <i>FT</i>	Turning, CBN – TNGA 160408 S01030	$v_c = 150$ m/min, $f = 0,06$ mm/obr, $a_p = 0.15$ mm
<i>Ball burnishing</i> <i>BR</i>	Burnishing using Si_3N_4 ceramic ball of 12 mm diameter	$v_c = 25$ m/min, $f_N = 0.025$ mm/obr, korekcja narzędzia 0,25 mm, load of 600 N
<i>Superfinish</i> <i>SF</i>	Superfinish using 99A320N10V ceramic honestone	Oscilation frequency of 680 osc/min, amplitude of 3.5 mm, load of 40 N

Measurements of surface profiles and surface topographies were carried out using a TOPO-01P contact profilometer equipped with a diamond stylus of $2\pm 0,5$ μm diameter. The determination of 2D and 3D surface roughness parameters and the visualization of all specific machined surfaces were done by means of Mountains Map v 6 program distributed by Digital Surf. In this comparative study the value of S_a (R_a) parameter was selected to be about 0.2 μm for all three machined surfaces (denote by symbols FT , BR and SF). For burnishing and superfinishing operations the initial surface (IT-initial turning) was turned to obtain the surface roughness of $R_a = 0.44$ μm (appropriate cutting parameters: $v_c = 150$ m/min, $f = 0.1$ mm/obr, $a_p = 0.15$ mm).

3. Experimental results

It is well known that from the practical point of view (from both construction and functional ones) the most important is the comparison of the average arithmetic surface height S_a and the maximum profile height S_z as provided in Fig. 2.

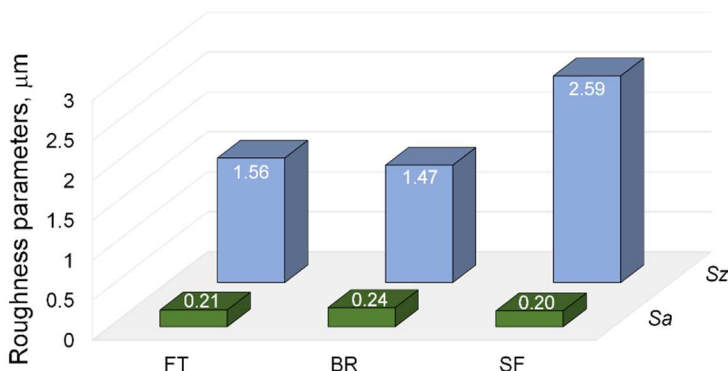


Fig. 2. Comparison of values of S_a and S_z roughness parameters for three machining operations

It should be noticed that all generated machined surfaces can be classified to the group of precise machining [11] because the values of S_z parameter are equal to $1,56$ μm , $1,47$ μm and $2,59$ μm for finish hard turning (FT), ball burnishing (BR) and superfinishing (SF) final operations. On the other hand the values of R_z parameter are close to 1 μm as shown in Fig. 3. They are presented in a bar diagram in Fig. 2. The main observation in Fig. 2 is that the S_z parameter depends on the type of machining operations performed.

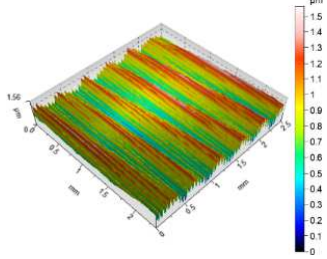
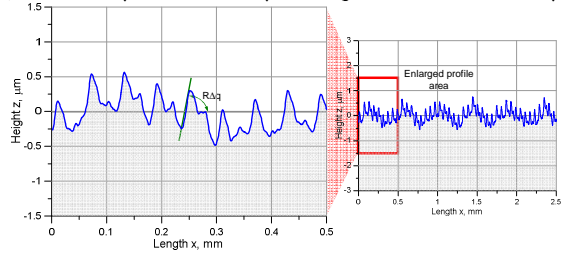
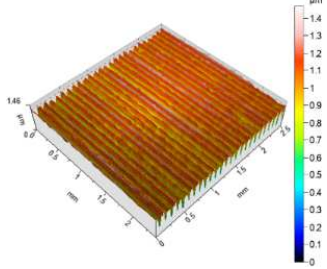
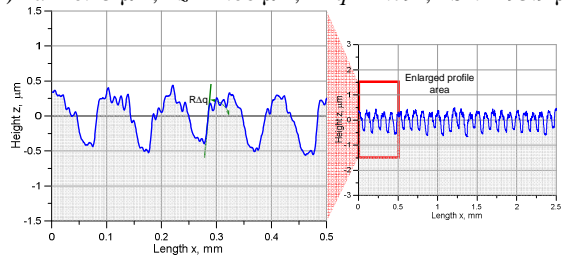
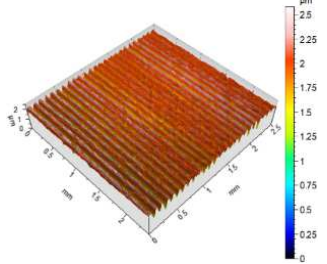
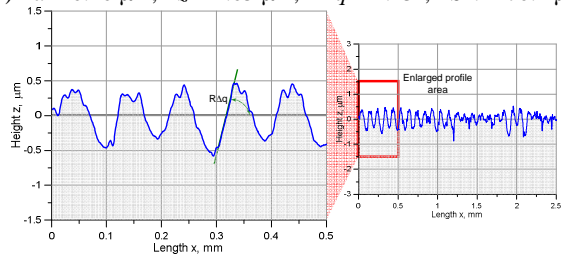
a1) $Sa = 0.21 \mu\text{m}$, $Sz = 1.56 \mu\text{m}$ a2) $Ra = 0.21 \mu\text{m}$, $Rz = 1.20 \mu\text{m}$, $R\Delta q = 1.62^\circ$, $RSm = 67.4 \mu\text{m}$ b1) $Sa = 0.24 \mu\text{m}$, $Sz = 1.47 \mu\text{m}$ b2) $Ra = 0.25 \mu\text{m}$, $Rz = 1.06 \mu\text{m}$, $R\Delta q = 1.79^\circ$, $RSm = 93.9 \mu\text{m}$ c1) $Sa = 0.20 \mu\text{m}$, $Sz = 2.59 \mu\text{m}$ c2) $Ra = 0.20 \mu\text{m}$, $Rz = 1.05 \mu\text{m}$, $R\Delta q = 1.43^\circ$, $RSm = 70.1 \mu\text{m}$ 

Fig. 3. Images of machined surfaces generated by hard turning (*FT*) (a1,2), ball burnishing (*BR*) (b1,2) and superfinishing (*SF*) (c1,2)

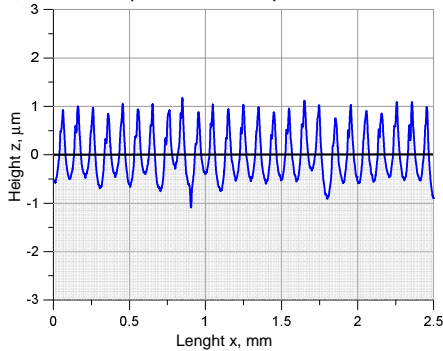
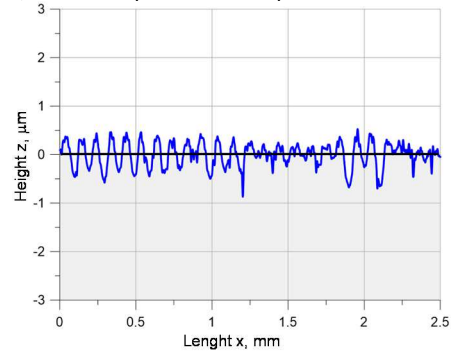
a) $Ra = 0.44 \mu\text{m}$, $Rz = 1.93 \mu\text{m}$ b) $Ra = 0.20 \mu\text{m}$, $Rz = 1.05 \mu\text{m}$ 

Fig. 4. Surface profiles obtained after initial turning *IT* (a) and subsequent superfinishing *SF* (b)

Characteristic surface topographies and surface profiles with comparable Sa/Ra values produced by removal and non-removal machining operations are shown in Fig. 3. It can be observed that surfaces after finish hard turning (Fig. 3a1,2) consists of a number of regularly distributed peaks and valleys which are visibly deformed after ball burnishing (Fig. 3b1,2). In consequence, the modified surface profile consists also of regularly distributed feed marks but with distinctly higher axial space ($RSm = 67.4 \mu\text{m}$ vs. $93.9 \mu\text{m}$) and local small peaks distributed along the main peaks. After superfinishing (Fig. 3c1,2) the surface irregularities are partially removed and new peaks with visible plateau are formed but the axial pitch is practically the same ($RSm = 67.4 \mu\text{m}$ vs. $70.1 \mu\text{m}$). This effect is presented in Fig. 4.

In terms of fractal analysis all machined surfaces can be classified as *multi-fractals* because they always contain some fragments of previous surfaces produced by hard turning. As a result, fractal analysis is able to detect all un-removed surface areas. The values of fractal dimension Sfd determining for machined surfaces presented in Fig. 3 are specified in a bar diagram in Fig. 5

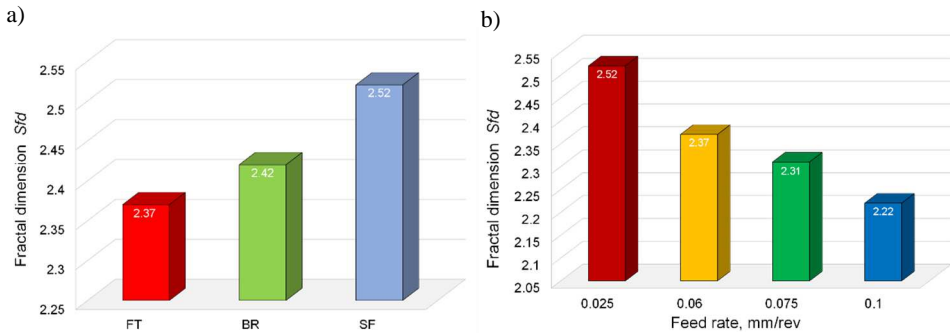


Fig. 5. Influence of machining operation on fractal dimension Sfd (a) and influence of feed rate for turning operations (b). Machining conditions: $Sfd = 2.52$ ($v_c = 150$ m/min, $f = 0.025$ mm/rev, $a_p = 0.03$ mm), $Sfd = 2.37$ ($v_c = 150$ m/min, $f = 0.06$ mm/rev, $a_p = 0.15$ mm), $Sfd = 2.31$ ($v_c = 150$ m/min, $f = 0.075$ mm/rev, $a_p = 0.15$ mm), $Sfd = 2.22$ ($v_c = 150$ m/min, $f = 0.1$ mm/rev, $a_p = 0.15$ mm)

The previous assumptions concerning fractal representation of the machined surfaces with different interactions between the tool and the workpiece surface are confirmed by the appropriate differences in the fractal dimension values. As suggested the highest difference in the Sfd values was determined for turned and superfinished surfaces ($Sfd = 2.37$ vs. 2.52) due to substantial modification of surface irregularities by abrasive grains. The modification of the turned surface in terms of fractal transformation (surface becomes less geometrically complex) by ball burnishing is not distinct due to high hardness of the workpiece material ($Sfd = 2.37$ vs. 2.42).

It can also be seen (Fig. 5b) that fractal dimension decreases when the feed rate increases. This effect is similar to the surface profile modification resulting from ball burnishing because the axial distance between peaks increases. For instance the value of Sfd decreases down to 2.22 when the feed rate increases up to 0.1 mm/rev.

Figure 6 presents a log-log diagram of relative areas versus scale for the three geometrical surface structures analyzed in this comparative study. The relative area is defined as the ratio of measured area to the predicted or nominal area. This diagram can be used for determining the fractal dimension ($D = 2$) and corresponding scale for which this dimension was used. It should be noticed that, in general, several fractal dimensions and corresponding scale can be determined on real multi-fractal surfaces generated during several technological passes. In particular, when the length of measured area is greater in relation to the characteristic topographic features both relative lengths and areas will approach. Assuming that the resolution of data will be less than topographic data the scale of a smooth-rough transition can be defined. This scale is characterized by the fact that above a smooth surface characterized by the Euclidean geometry exists but below it a rough surface which can be characterized by means of fractal geometry [11].

In the case study shown in Fig. 6 a strong correlation between the values of fractal dimension and relative areas for the scale equal to $70 \mu\text{m}^2$ can be observed [12].

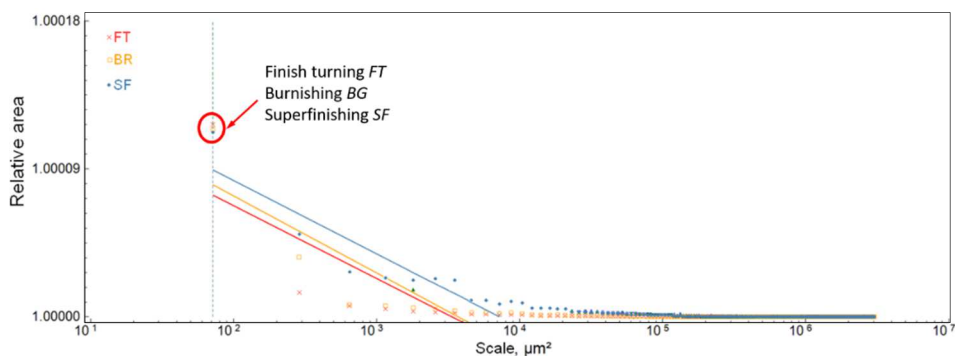


Fig. 6. Comparison of fractal dimension for geometrical surface structures using log (relative area)-log (scale) diagram

When analyzing the geometric structure of the surface with PSD, we must take into account that the PSD is the square of the amplitude value of the profile/surface roughness as a function of the wavelength. As a result, one has the opportunity to quantify the process depending on the frequency and direction of analysis [13].

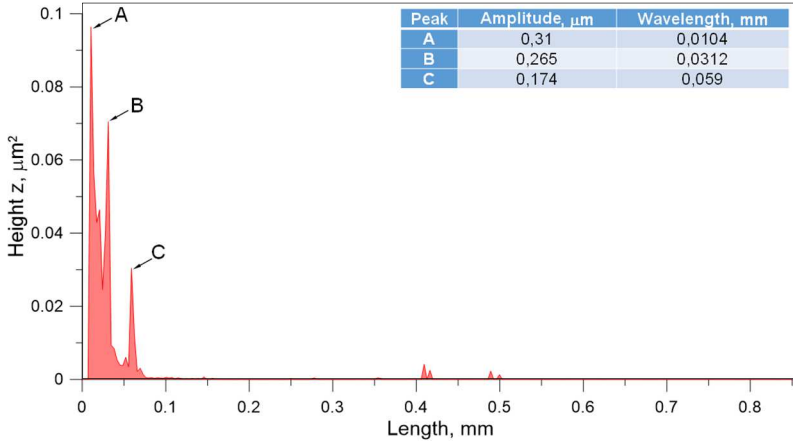


Fig. 7. Power spectral density for surface after turning *FT*

Figure 7 shows the power spectral density after dry turning *FT* of steel with the parameters $v_c = 150$ m/min, $f = 0.06$ mm/rev and $a_p = 0.15$ mm. The maximum vibration amplitude in this case is $0.31 \mu\text{m}$ (peak A). It should be added here that an additional smaller peak B with an amplitude of $0.265 \mu\text{m}$ and a wavelength of 0.0312 mm can be caused, as mentioned earlier, by the plastic flow effect of the material during turning and chip segmentation. The wavelength of C peak of 0.059 mm represents the feed rate (0.06 mm/rev).

Before starting the frequency analysis for the surface after burnishing and superfinishing, the PSD spectra should be analyzed for surfaces after turning ($v_c = 150$ m/min, $f = 0.1$ mm/rev, $a_p = 0.15$ mm) (Fig. 8), which was the initial surface for subsequent burnishing operations (*BR*) and superfinishing (*SF*). After preliminary turning (*IT*), Fig. 8, the distribution of the power spectral density is

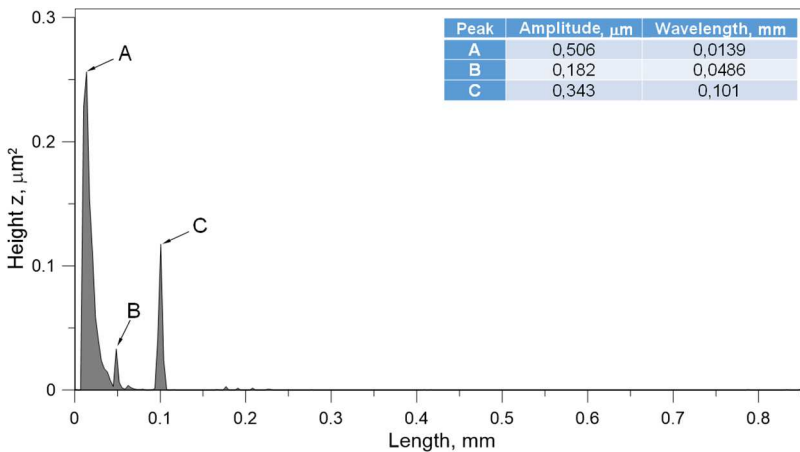
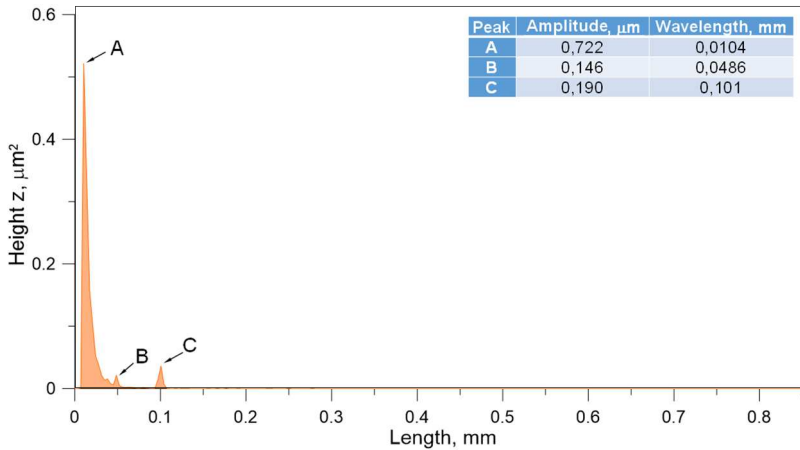
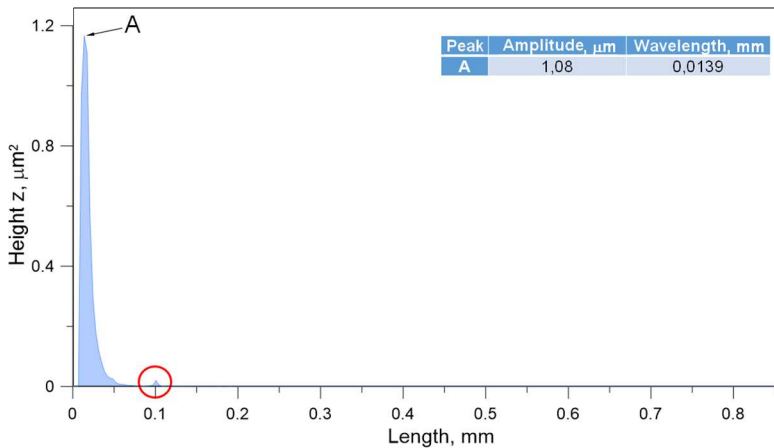


Fig. 8. Power spectral density for surface after preliminary turning *T*

Fig. 9. Power spectral density for the surface after burnishing *BR*Fig. 10. Power spectral density for the surface after superfinishing *SF*

dominated by one component with a wavelength of 0.0139 mm and an amplitude of 0.506 μm (peak A), concentrated in one frequency range. Peak C, whose wavelength is 0.101 mm, represents the feed rate (0.1 mm/rev).

After burnishing (*BR*) with 600 N force (Fig. 9), the main component (peak A) increased by about 40%, which may be caused by surface smoothing, while the higher order components marked as B and C peaks (were smoothed in the range 25% (B) and 80% (C)). This may indicate a signal flow towards low frequencies.

In the superfinishing (*SF*) (Fig. 10), a much larger increase in the main component (peak A) by about 110% was recorded compared to the burnishing process, this is due to the smoothing of the surface as after burnishing (Fig. 9) and

the use of a tool that there is a hone. However, the remaining one component of the higher order marked in red, which is a residue after turning ($f = 0.1$ mm/rev), was smoothed in comparison with an output amplitude of $0.334 \mu\text{m}$ to approximately $0.021 \mu\text{m}$. Similarly to the burnishing process, this may indicate the signal shift towards low frequencies.

4. Summary

This paper reveals some practical possibilities for using the fractal dimension and the PSD as metrics for assessing the geometrical states of machined surfaces generated during removal and non-removal operations. It was documented that the fractal dimension is the highest for superfinished surfaces in comparison to turned and subsequently burnished surfaces due to their lower geometrical complexity and irregularity (also randomness). In addition, it was documented that the fractals and surface roughness parameters exhibit so-called the concurrency of opposition, which means that higher fractal dimension corresponds to lower values of the R_z roughness parameter (moreover the higher peak density S_{ds} correlates with higher surface complexity). The analysis of the frequency spectrum using the FFT transform can be used to detect some residual areas remained from the initial (turning) operations on the finished surfaces (after burnishing or superfinishing). This specific technological problem is very complex but it should be considered when generating the functional engineered surfaces.

References

- [1] W. GRZESIK: Wpływ topografii powierzchni na właściwości eksploatacyjne części maszyn. *Mechanik*, **88**(2015)8-9.
- [2] T. BURAKOWSKI: Areologia. Podstawy teoretyczne, Wydawnictwo Naukowe Instytutu Technologii Eksploatacji – Państwowy Instytut Badawczy, Radom 2013.
- [3] P. PAWLUS: Topografia powierzchni, pomiar, analiza, oddziaływanie, Oficyna Wydawnicza Politechniki Rzeszowskiej, Rzeszów 2006.
- [4] K.E. OCZOŚ, V. LIUBIMOV: Struktura geometryczna powierzchni. Podstawy klasyfikacji z atlasem charakterystyk powierzchni kształtowanych, Oficyna Wydawnicza Politechniki Rzeszowskiej, Rzeszów 2003.
- [5] M. WIECZOROWSKI: Metrologia nierówności powierzchni, metody i systemy, Wydawnictwo ZAPOL, Szczecin 2013.
- [6] K. ŻAK, RZAŚA M.: Wykorzystanie wymiaru fraktalnego do identyfikacji podobieństwa powierzchni. *Mechanik*, **85**(2012), 1868-1869.
- [7] WHITEHOUSE D.J.: Fractal or fiction. *Wear*, **249**(2001), 345-353.
- [8] WIECZOROWSKI M., Wykorzystanie analizy topograficznej w pomiarach nierówności powierzchni, Wydawnictwo Politechniki Poznańskiej, Nr 429, Rozprawy, Poznań 2009.

- [9] HASEGAWA M., LIU, J., OKUDA K., NUNOBIKI M.: Calculation of the fractal dimensions of machined surface profiles. *Wear*, **192**(1996), 40-45.
- [10] GRZESIK W., RECH J., ŽAK K.: Characterization of surface textures generated on hardened steel parts in high-precision machining operations. *International Journal of Advanced Manufacturing Technology*, **78**(2015)9-12, 2049-2056.
- [11] BROWN Ch.A., JOHNSEN W.A., HULT K.M.: Scale-sensitivity, Fractal analysis and simulations. *International Journal Machine Tools and Manufacture*, **38**(1998)5-6, 633-637.
- [12] ŽAK K.: Areal field and fractal based characterization of hard surfaces produced by different machining operations, *Journal of Machine Engineering*, **16**(2016)1, 24-32.
- [13] ŽAK K.: Influence of grinding conditions on the topographic characteristic of machined surfaces. *Journal of Machine Engineering*, **14**(2014)2, 47-56.

Received in December 2017

